J Appl Physiol 127: 1067–1074, 2019.
First published August 22, 2019; doi:10.1152/japplphysiol.01100.2018.

INNOVATIVE METHODOLOGY

Deriving the arterial P_{O_2} and oxygen deficit from expired gas and pulse oximetry

G. Kim Prisk and John B. West

Department of Medicine, University of California, San Diego, La Jolla, California

Submitted 12 December 2018; accepted in final form 19 August 2019

Prisk GK, West JB. Deriving the arterial P_{O_2} and oxygen deficit from expired gas and pulse oximetry. *J Appl Physiol* 127: 1067–1074, 2019. First published August 22, 2019; doi:10.1152/japplphysiol.01100.2018.—The efficiency of pulmonary gas exchange is often assessed by the ideal alveolar-arterial partial pressure difference (A-aDO_2). Through a combination of pulse oximetry and rapidly responding gas analyzers to measure the partial pressures of O_2 and CO_2 in expired gas, one can measure the oxygen deficit. Defined as the difference between the measured alveolar P_{O_2} and the arterial P_{O_2} calculated from Sp_{O_2}, the oxygen deficit is a substitute for the alveolar-arterial P_{O_2} difference. The oxygen deficit is physiologically reasonable in that it increases with age in healthy subjects and is well correlated with the A-aDO_2. To calculate arterial P_{O_2} from saturation, the saturation should be below the very flat upper part of the O_2-Hb dissociation curve; good estimates can be made provided the arterial O_2 saturation is below ~95%. Since saturations at or above 95% imply reasonably well-maintained gas exchange efficiency, this limitation is of only minor concern. Calculations show that it is necessary to take into account the change in P_{O_2} at a saturation of 50% of the O_2-Hb dissociation curve based on the measured alveolar P_{CO_2}. As the measurement is designed to be noninvasive, determination of any base excess is not practical, but calculations show that the effect of assuming a zero base excess is modest, with a similar small effect from an abnormal body temperature. Taken together, these results show that a noninvasive assessment of pulmonary gas exchange efficiency can be obtained from subjects with below-normal arterial O_2 saturations through a combination of expired O_2 and CO_2 measurements and Sp_{O_2} made during quiet breathing.

NEW & NOTEWORTHY The details and limitations of a noninvasive measurement of pulmonary gas exchange efficiency, the oxygen deficit, are described. The oxygen deficit, calculated from expired gas measurements made during quiet breathing coupled with pulse oximetry, is a good surrogate measurement of the ideal alveolar-arterial P_{O_2} difference and does not require arterial blood gas sampling.

alveolar-arterial O_2 difference; blood gases; expired gas; gas exchange

INTRODUCTION

Assessing gas exchange efficiency in patients is an important aspect of clinical management. This has progressed from what could be determined by physical examination and the observation of cyanosis and has been greatly advanced by the development of blood gas electrodes and pulse oximetry. Today, it is commonplace to have the arterial oxygen saturation measured as often as systemic blood pressure during clinician encounters. This is a direct consequence of the rapid development and miniaturization of the arterial pulse oximeter, which can now be obtained as a battery-powered device that can be applied to a fingertip with a result obtained in 15 s or less in a completely noninvasive manner.

It is well appreciated that knowledge of the arterial saturation from a pulse oximeter (Sp_{O_2}) is an incomplete measure of pulmonary gas exchange status, and if a more detailed picture is required, then more comprehensive measurements are necessary. Typically, these measurements involve the collection of an arterial blood sample drawn anaerobically and subsequently analyzed to determine the partial pressures of oxygen and carbon dioxide, the pH, and the base excess. Together, these parameters provide a comprehensive picture of pulmonary gas exchange. Furthermore, based on the arterial P_{O_2} and P_{CO_2}, the well-established alveolar-arterial oxygen difference (A-aDO_2) can readily be calculated. This uses the construct of "ideal alveolar gas" introduced by Riley and Cournand (13), and the A-aDO_2 is considered as a useful measure reflecting the impairment in pulmonary gas exchange that results from ventilation-perfusion inequality in the lung (16).

However, arterial blood sampling is invasive, at times uncomfortable for the patient, requires specialized skills, is time consuming, and expensive. We considered that it would be potentially useful to be able to measure a surrogate for the A-aDO_2 in a noninvasive and rapid manner. Our method, which has been shown to provide a potentially useful insight into pulmonary gas exchange, utilizes the combined measurement of arterial oxygen saturation from a pulse oximeter and measurement of the end-tidal oxygen and carbon dioxide partial pressures during quiet breathing. From this we calculate the "oxygen deficit," which can be thought of as an analogous measurement to the A-aDO_2 (described in detail below). We have shown in prior publications that the oxygen deficit is very small in young healthy subjects under conditions of hypoxia, somewhat larger in older but otherwise healthy adults (19) also in hypoxia, and considerably elevated in patients with a variety of pulmonary diseases (20). The oxygen deficit is well correlated with the A-aDO_2 measured using an arterial blood gas sample in patients (16). Furthermore, the estimated values of both arterial P_{O_2} and P_{CO_2} measured noninvasively correlate well with directly measured arterial blood gas values in patients (20).

Since, based on these prior studies, it appears that the noninvasive measurement of oxygen deficit is both practical and potentially useful (9), it is important that the details of the technique are well understood, the physiological basis of the

Address for reprint requests and other correspondence: G. Kim Prisk, Dept. of Medicine-0852, Univ. of California, San Diego, 9500 Gilman Dr., La Jolla, CA 92093-0852 (e-mail: kprisk@ucsd.edu).

measurement is clear, and the limitations that exist are stated. Although the prior studies referred to above have outlined the measurement technique, this paper aims to provide a comprehensive description on estimating gas exchange defects using expired gas measurements and provide clarity on the limitations of such an approach.

METHODS

Estimating the oxygen deficit requires the measurement of end-tidal O_2 and CO_2 from expired gas measurements and the derivation of arterial P_{O_2} from pulse oximetry.

Measuring End-Tidal O_2 and CO_2

End-tidal measurements of gas concentrations (or partial pressures) require rapidly responding gas analyzers to accurately capture the changing expired concentrations of O_2 (falling) and CO_2 (rising) throughout expiration. Previous studies have shown that a response time (10%–90%) of ~100–150 ms is adequate to accurately determine the exhaled breath profile arising from resting breathing (2). In this case, the device uses separate O_2 and CO_2 analyzers (available from several manufacturers), each with a response time of ~130 ms and 100 ms from 10% to 90% (respectively). Typical output from these analyzers is shown in Fig. 1. These data were derived from a patient with lung disease, wearing a nose clip, and breathing air quietly through a mouthpiece. The tip of the gas sampling tube was inserted through the side wall of the mouthpiece so that gas was sampled from the middle of the gas flow. The gas sampling line includes Nafion to equilibrate the water vapor content of the sampled gas with ambient conditions to eliminate the dependency of the analyzer output on humidity, as recommended by the manufacturers of the gas analyzers.

End-tidal values were determined by detecting the rapid fall in CO_2 and rise in O_2 that occurred at the onset of inspiration as fresh inspired air was brought to the tip of the sampling tube.

The data in the 0.5 s preceding this point were then averaged to produce the end-tidal values for O_2 and CO_2 for that breath, incorporating approximately the last one-fifth of the expiration at a normal respiratory rate. These are plotted in the lower section of Fig. 1 as a trend plot with a single value per breath plotted. This trend plot provides a visual indication of the degree of steady-state breathing being produced by the patient. The aim is to have all the end-tidal values derived from breaths that are of comparable tidal volume and which all end at functional residual capacity. To help ensure this, an indication of steady-state breathing was determined by considering the variation in end-tidal CO_2 over the preceding 45 s. This results in the steady-state indicator being set as shown in the lower right corner of Fig. 1. The average of the end-tidal O_2 and CO_2 values over the last five breaths are shown in the top left corner of Fig. 1. Partial pressures are derived based on the measured concentrations and the measured barometric pressure (Fig. 1, *top right middle*).

A frequent objection to using the end-tidal partial pressures as a measure of alveolar partial pressures is that their values depend on the duration of expiration. If the duration is increased, the P_{O_2} continues to fall and the P_{CO_2} continues to rise. However, evidence shows that the end-tidal P_{O_2} is a robust measurement if a steady state has been obtained (19). In brief, the end-tidal P_{O_2} is taken as the value in the alveolar gas at the end of a relaxed expiration or the lung volume just above this. The end expiratory lung volume is a very repeatable measurement under steady-state conditions, being determined by the elastic recoil properties of the lung and the chest wall.

Deriving the Arterial P_{O_2} from the Sp_{O_2}

The O_2-Hb dissociation curve is well known, and we routinely estimate saturation from P_{O_2} measurements. In the present situation, we take the inverse approach, and, based on the arterial O_2 saturation from a pulse oximeter, we calculate the P_{O_2} in the arterial blood.

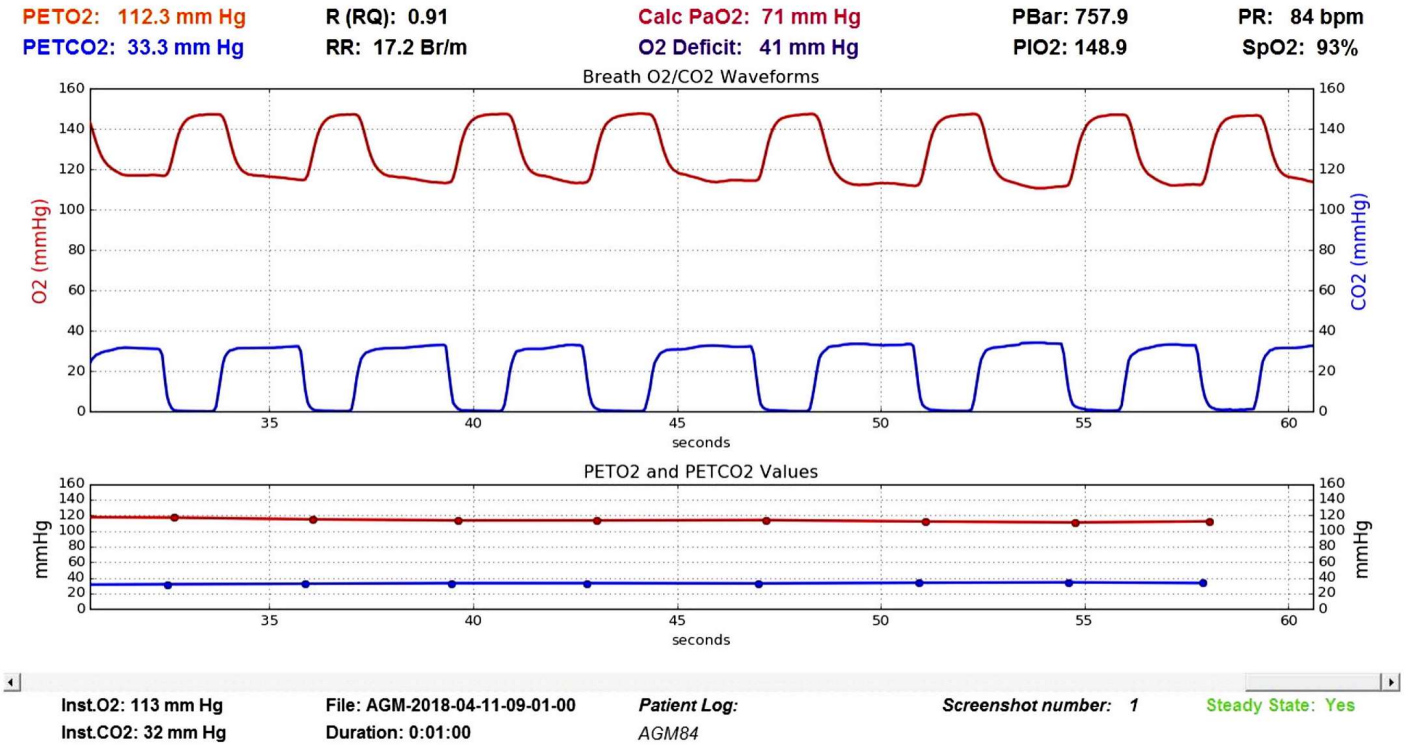

Fig. 1. Output from a prototype gas exchange monitor. The image is a screenshot of the device when in use on a patient with lung disease breathing air. Note that the rapidly responding analyzers provide a good record of the inspired and expired waveforms of O_2 and CO_2. The trend plot in the lower portion of the screen allows assessment of steady state, and this is also indicated by the stability of end-tidal values and is indicated at the *bottom right*. PBar, barometric pressure; PETCO2, end-tidal partial pressure of carbon dioxide; PETO2, end-tidal partial pressure of oxygen.

Doing so requires 2 steps: first, the P_{O_2} at a saturation of 50% (P50) of the O_2-Hb dissociation curve must be determined, and second, an inverse form of the relationship between P_{O_2} and saturation must be used to calculate the P_{O_2}.

The O_2-Hb dissociation curve shifts to the left or to the right as a result of changes in P_{CO_2} (the Bohr effect), pH, temperature, and 2,3-diphosphoglycerate. However, by far the biggest shift is that arising from changes in P_{CO_2}, as discussed in the section on the magnitude of the Bohr effect (in RESULTS section, below). Although the other effects are not unimportant, they are not information that is readily available in most instances.

We used the end-tidal P_{CO_2} (measurement described above) as a measure of arterial P_{CO_2}. It is well established that by virtue of the flatness of the blood R line in the O_2-CO_2 diagram that end-tidal P_{CO_2} and arterial P_{CO_2} values are equivalent (3), and indeed, the calculation of the widely used ideal A-aDO_2 uses that assumption (1). We estimated the P50 of the O_2-Hb dissociation curve using the Kelman routines (18). These are based on the results of published biochemical studies of the effects of changing the appropriate variables. These were applied for varying values of P_{CO_2} under the assumption that the base excess was zero and the temperature was 37°C.

Inverting the relationship between P_{O_2} and saturation (i.e., calculating P_{O_2} based on saturation) was based on the inversion of the Hill equation: $P_{O_2}{}^n = P50^n \times Sa_{O_2}/(1 - Sa_{O_2})$. This form is readily solved digitally without inverting the equation by taking the logarithm of the equation and solving algebraically.

Oxygen Deficit

The oxygen deficit was derived as the difference between the end-tidal P_{O_2} measured as described above (that is, the averaged end-tidal value over the last five breaths), and the calculated arterial P_{O_2} also described above. Using the same algorithm as that incorporated in the commercial device for measuring the oxygen deficit, we first examined the effects of the errors that result from incorrect assumption of a zero base excess and from the assumption of a normal body temperature (37°C) on the calculated oxygen deficit. These represent "static" errors that would serve to make for consistent error in measurements performed on a particular subject.

Monte Carlo Simulation of the Oxygen Deficit

The sensitivity of the calculated oxygen deficit to errors in measured Sp_{O_2} from the pulse oximeter and to errors in the measured values of end-tidal O_2 and CO_2 (together, these 3 parameters are used to calculate the oxygen deficit) was assessed by considering the effect of simultaneous assumed errors in all three using a Monte Carlo approach.

Using a fixed reference point of a PA_{O_2} of 100 mmHg, and a PA_{CO_2} of 40 mmHg, 200 uniformly distributed values of Pa_{O_2} in the range for 40–100 mmHg were used as the input and the corresponding nominal fractional saturation values calculated using the Kelman routines. For each of these points, normally distributed random errors in fractional saturation and end-tidal P_{O_2} and P_{CO_2} were generated a total of 1,000 times, and each such set of values was used as input parameters to the algorithm used to calculate Pa_{O_2} and, subsequently, the oxygen deficit. Random errors that resulted in fractional saturation values of >0.995 were replaced by a value of 0.995. Thus, for a given value of fractional saturation, the result was a mean value of the oxygen deficit, and its associated standard deviation.

To provide realistic values of the errors in fractional saturation and in end-tidal gases, we determined the variability in individuals of these input parameters in a data set collected with the commercial device. The data were from 37 normal subjects ranging in age from 20 to 91, totaling 597 separate measurements (~16 per subject). Four values of FI_{O_2} were used (0.21, 0.175, 0.15, and 0.125). Fractional saturation showed a standard deviation of 0.008 and was slightly higher at lower values of saturation. End-tidal P_{O_2} showed a standard deviation of 2.7 mmHg, and end-tidal P_{CO_2} showed a standard deviation of 1.03 mmHg.

Based on these figures and noting that prior studies have shown that many oximeters operate in the range of 2% accuracy (7), we increased the standard deviation of the fractional saturation to 0.01 units independent of the baseline value of fractional saturation. For end-tidal P_{O_2} and P_{CO_2}, we used standard deviation values of 3.3% and 2.7% of the value, respectively.

The Monte Carlo simulations considered simultaneous errors in O_2 and CO_2, in which the deviation was assumed to be in opposite directions. This was designed to be representative of a situation in which the fluctuations in O_2 and CO_2 resulted from physiological changes in end-tidal gas concentrations in which a reduction in O_2 is associated with an increase in CO_2 of similar magnitude (depending on the respiratory exchange ratio).

RESULTS

Deriving Arterial P_{O_2} from Sp_{O_2}

To calculate P_{O_2} from arterial saturation, two steps are required. First, the P50 of the O_2-Hb dissociation curve must be determined, as this varies as a result of changes in P_{CO_2} (the Bohr effect). Second, the Hill equation must be inverted using the newly derived value of P50.

Figure 2 plots a family of dissociation curves in which each curve results from a different value of P_{CO_2} and base excess is assumed to be zero. The values of P_{CO_2} are indicated for three curves. The intersection of each curve and the horizontal line shown at a fractional saturation of 0.50 is the P50 for that case, and these are shown for the most likely physiological values of P_{CO_2} (20–60 mmHg). The relationship is approximately linear, with P50 increasing by ~2.2 mmHg for each 10-mmHg increase in P_{CO_2}.

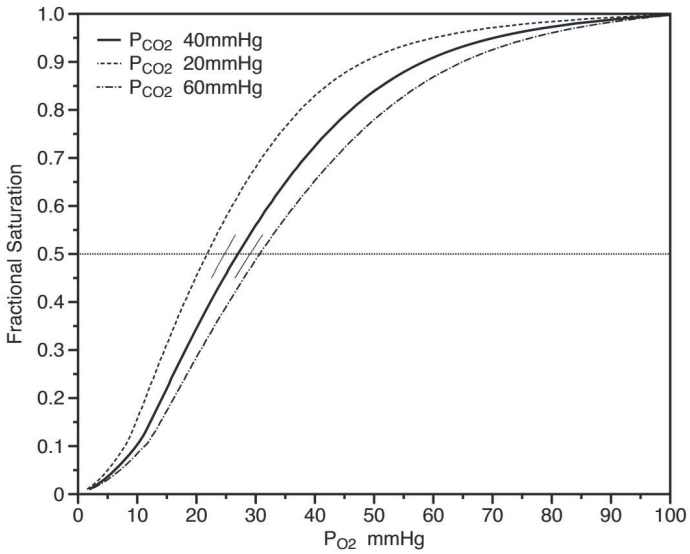

Fig. 2. A family of O_2-Hb dissociation curves for varying values of P_{CO_2} between 20 mmHg and 60 mmHg calculated using the Kelman routines (18). The standard dissociation curve (P_{CO_2} 40 mmHg) has a P_{O_2} at a saturation of 50% (P50) of 27 mmHg and is plotted as the heavier black line. For clarity, dissociation curves for intermediate values of P_{CO_2} are plotted only over the fractional saturation range of 0.45 to 0.55 (the short lines). The lines assume a zero value for the base excess and a temperature of 37°C. The point where each curve crosses the horizontal line at a fractional saturation of 0.5 is the P50.

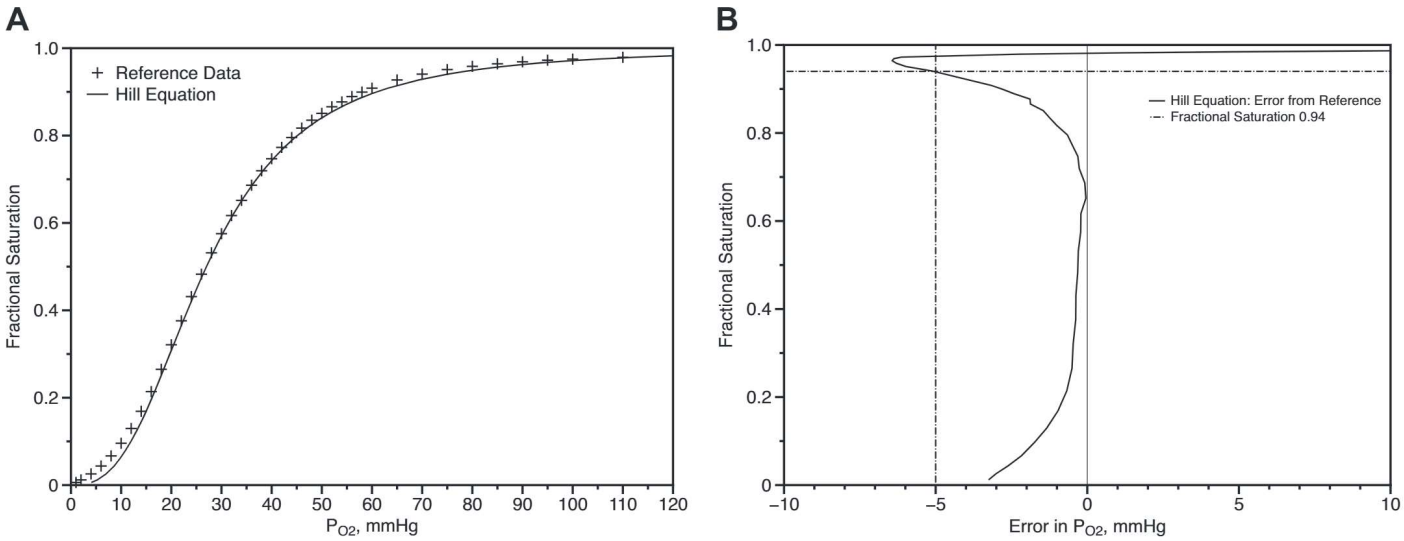

Fig. 3. *A*: the O_2-Hb dissociation curve calculated from solving the Hill equation for different values of fractional saturation assuming P_{O_2} at a saturation of 50% of 27 mmHg and a Hill coefficient of 2.7 (solid line). The crosses are published reference values for the P_{O_2} saturation relationship under standard conditions (14). *B*: the error in calculated P_{O_2} from *A* compared with the reference data in *A*. Note that for the purposes of comparison with *A*, fractional saturation (the independent variable) is plotted vertically, and the error in P_{O_2} (the dependent variable) is plotted horizontally. The horizontal line at a fractional saturation of 0.94 indicates the region above which the error in calculated P_{O_2} varies by more than 5 mmHg from the reference data and indicates the region in which the calculation of P_{O_2} from Sp_{O_2} gives results that may not be useful.

Figure 3*A* shows the dissociation curve that results from calculating the P_{O_2} from saturation via the Hill equation using a Hill coefficient (the "n" in the equation) of 2.7 and a P50 of 27 mmHg. Also shown in Fig. 3*A* (crosses) are a series of measurements of reference values for P_{O_2} and saturation published by Severinghaus (14) for "standard conditions" (7.40 pH, temperature = 37°C). Figure 3*B* shows the error in calculated P_{O_2} compared with these reference data. Note that for values below a fractional saturation of 0.95, the error is <5 mmHg.

Magnitude of Changes in P_{CO_2} on Calculated P_{O_2}

As Fig. 2 shows, alterations in the arterial P_{CO_2} result in a shift of the O_2-Hb dissociation curve (the Bohr effect). Figure 4 shows the magnitude of the error in calculated P_{O_2} that results from ignoring the Bohr effect. In other words, if the change in P50 resulting from a change in P_{CO_2} shown in Fig. 2 was not included, then there would be a resulting error in calculated P_{O_2}. The magnitude of this error is dependent on Sp_{O_2}, and Fig. 4 shows that for values of fractional saturation that are most commonly encountered (say between 0.60 and 0.98), the effect is to underestimate P_{O_2} if the P_{CO_2} is low and to overestimate the P_{O_2} if the P_{CO_2} is high. The magnitude of these errors is more than 5 mmHg in the calculated P_{O_2} for a large (10 mmHg) change in P_{CO_2} at higher saturation values.

Magnitude of the Effect of a Nonzero Base Excess on Calculated P_{O_2}

The magnitude of a nonzero base excess was estimated by using the Kelman routines to calculate the effect of a change in base excess on the P50 of the O_2-Hb dissociation curve. The results are shown in Fig. 5, which shows the change in P50 from its nominal value when the value for the base excess was raised or lowered, all other effects being held constant. It can be seen that the effect is asymmetric with a base excess of 10 mEq/L lowering the P50 by ~1.7 mmHg and a base deficit of 10 mEq/L raising the P50 by ~4.8 mmHg. Thus, the effect of a large base deficit of 10 mEq/L would result in a right shift of the O_2-Hb dissociation curve of 4.8 mmHg, equivalent to an error in P_{CO_2} of ~22 mmHg (based on Fig. 2). This in turn would result in an error in calculated P_{O_2} of ~8 mmHg at a fractional saturation of 0.90 (based on Fig. 4). In contrast, a base excess of 10 mEq/L would be the equivalent of a ~−7 mmHg change in P_{CO_2} (Fig. 2), with a resulting error in P_{O_2} of ~−3 mmHg at a fractional saturation of 0.90 (Fig. 4).

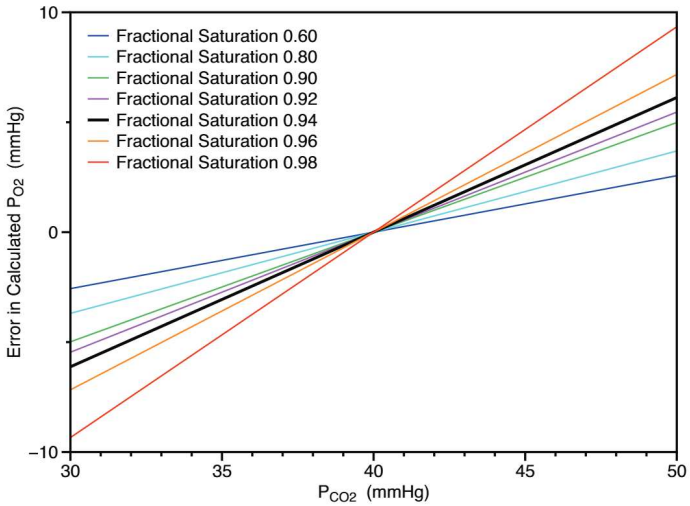

Fig. 4. The effect of ignoring the change in P_{O_2} at a saturation of 50% resulting from a value of P_{CO_2} that is different from the nominal value of 40 mmHg on the calculated P_{O_2}. Note that the magnitude of the error increases as Sp_{O_2} increases. For fractional saturation values of 0.94 (the thick bolded black line in the figure) or below, the magnitude of the resulting error in P_{O_2} remains below approximately ±5 mmHg for errors in P_{CO_2} of up to ±10 mmHg.

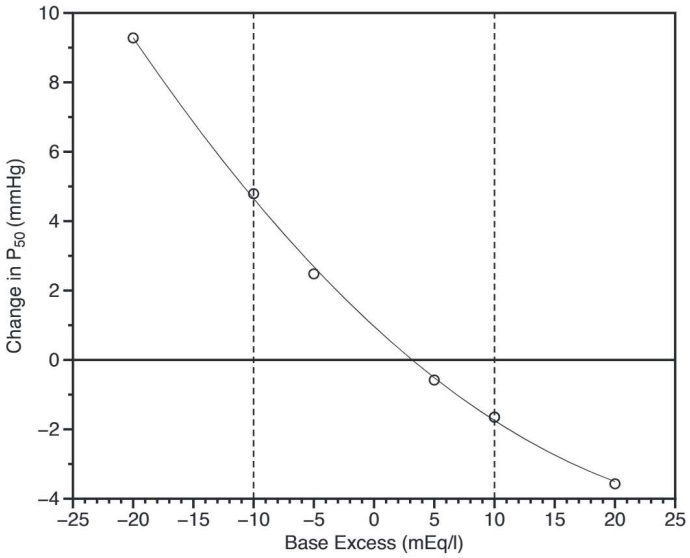

Fig. 5. Change in P_{O_2} at a saturation of 50% (P50) resulting from a nonzero base excess. A base excess of +10 mEq/L reduces P50 by ~2 mmHg, whereas a base deficit of 10 mEq/L (base excess of −10 mEq/L) causes P50 to increase by ~4.8 mmHg (indicated by the vertical lines). See text for details.

Magnitude of the Effect of Altered Body Temperature on Calculated P_{O_2}

All the calculations performed above used a standard body temperature of 37°C in the Kelman routines. However, circumstances might occur in which body temperature differs from this (e.g., a fever). The P50 changes approximately linearly with temperature, increasing by ~1.7 mmHg per degree Celsius. Thus, for purposes of scale, a body temperature of (say) 39°C would raise P50 by 3.4 mmHg, equivalent to an error in P_{CO_2} of ~15 mmHg (based on Fig. 2), which would serve to increase P_{O_2} by ~3.5 mmHg (based on Fig. 4).

Monte Carlo Analysis of Oxygen Deficit to Errors in the Contributing Measurements

Given the flatness of the O_2-Hb dissociation curve at fractional saturation values at or above 0.95, the most likely source of variability in the oxygen deficit is error in measured saturation. These errors would be expected to increase at higher values of saturation. Figure 6 shows the results of the Monte Carlo analysis for the calculation of oxygen deficit based on errors in measured fractional saturation of 0.01 (SD) and incorporating simultaneous and opposite direction errors (the worst-case scenario) of 3.3% (SD) in O_2 and 2.7% (SD) in CO_2.

There is a negative bias in the oxygen deficit that becomes apparent above a fractional saturation of ~0.85. Similarly, as saturation rises, the variability increases as the flat upper portion of the O_2-Hb dissociation curve is reached. At lower values of fractional saturation, the errors in oxygen deficit remain essentially constant until a value of ~0.90 is reached, at which point the SD of the oxygen deficit begins to increase. At fractional saturation values above ~0.95, the errors in oxygen deficit become large and rapidly increase. Figure 7 shows the relationship between the calculated oxygen deficit and the A-aDO_2 used as input to the Monte Carlo simulation.

DISCUSSION

The major message from this paper is that obtaining a reliable estimate of the oxygen deficit based upon noninvasive measurements of expired gases and arterial oxygen saturation from a pulse oximeter is both practical and can provide valuable results. However, the shape of the O_2-Hb dissociation curve, which is nearly flat at high values of P_{O_2}, means that estimates of the oxygen deficit (which depends on the calculated arterial P_{O_2}) are both biased and highly variable at fractional saturation values of ~0.95 or above. Both effects are a direct result of the flat upper portion of the O_2-Hb dissociation curve, with small differences in saturation resulting in large change in calculated P_{O_2}, and with the bias resulting from the fact that random errors in saturation cannot result in saturation values of >100%, skewing the resulting distribution of P_{O_2} and thus oxygen deficit. Furthermore, as shown in Fig. 3*B*, at fractional saturation values above ~0.85, the Hill equation underestimates fractional saturation, adding to this negative bias.

At lower values of fractional saturation (below ~0.85%), the primary source of error in the calculation of oxygen deficit results not from the calculation of Pa_{O_2} from fractional satura-

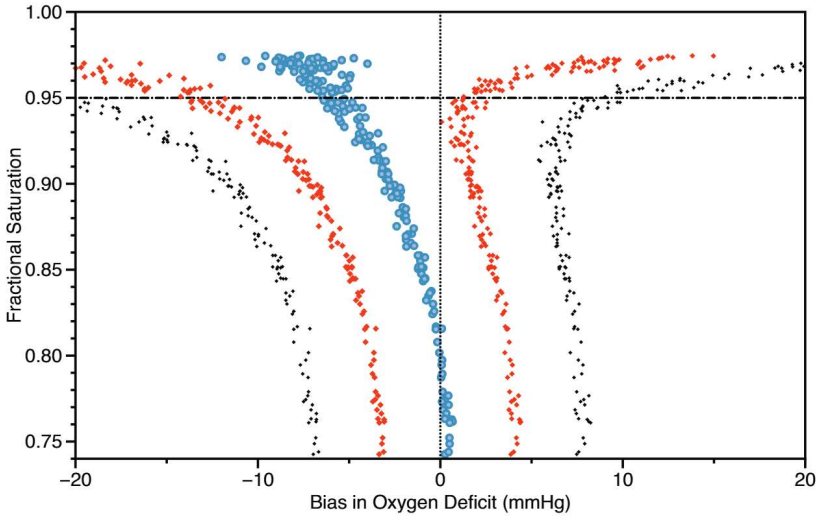

Fig. 6. The bias and error in oxygen deficit resulting from errors in the measurement of fractional saturation coupled with simultaneous error in the measurement of end-tidal O_2 and CO_2 in the opposite direction (a worst-case scenario). A Monte Carlo simulation of 1,000 points was used for each value of fractional saturation to determine the mean bias in the oxygen deficit, and its associated SD (see text for details). For each of the 200 values of fractional saturation (the *y*-axis), the mean bias in oxygen deficit is shown in blue, and the bias ±1 SD is shown in red. The black symbols show the mean bias ±1.96 SD (the 95% confidence interval). The vertical dotted line shows the case of zero bias. The horizontal dashed line at a fractional saturation of 0.95 shows that for fractional saturations above that, useful estimates of the oxygen deficit may not be practical.

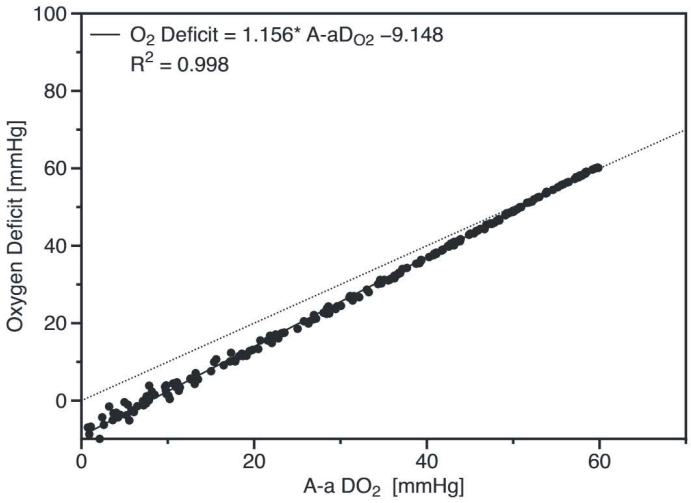

Fig. 7. Calculated oxygen deficit plotted as a function of the alveolar-arterial partial pressure difference (A-aDO_2) used as the input value to the Monte Carlo simulation. As indicated in Fig. 6, at higher values of fractional saturation, and thus at low values of the A-aDO2, a bias in calculated Pa_{O_2} results, and this leads to deviation from the line of identity (the dotted line).

tion but from the errors in the measurement of end-tidal O_2 and CO_2. This result is based on Monte Carlo simulations (not shown) in which differing levels of error in the input parameters were used, allowing the individual effects of each error source to be assessed.

Comparison of the Oxygen Deficit with the Ideal A-aDO_2

A classical means of assessing the efficiency of pulmonary gas exchange is the ideal alveolar-arterial O_2 difference. In the context of this paper, it is important to understand that although this is a well-accepted means of assessing pulmonary gas exchange, it relies on the artificial construct of ideal alveolar gas, a concept introduced by Riley and Cournand (13). This is estimated based on the measurement of the arterial P_{CO_2}, on the assumption that this is the same as the ideal alveolar P_{CO_2} because the blood R line on the O_2–CO_2 diagram is so nearly flat, on an assumed respiratory exchange ratio, and long established (3). The measured arterial P_{O_2} is then subtracted from this calculated value to yield the A-aDO_2. This is illustrated in figure 4 of Ref. 16.

In contrast, the oxygen deficit is based on a somewhat different construct in which the alveolar point is taken to be that measured as the end-tidal gas partial pressures. The arterial point is that calculated from the measured Sp_{O_2} with an appropriate correction for P_{CO_2} (the Bohr effect) based on the assumption that end-tidal P_{CO_2} is the same as arterial P_{CO_2}, something that has long been established (3). The difference between the end-tidal (alveolar) point and the calculated arterial is the oxygen deficit. Thus, the oxygen deficit includes both deviations from the ideal point resulting from areas of low ratio of ventilation to perfusion ($\dot{V}_A/\dot{Q}$), which are also included in the ideal A-aDO_2, and deviations from the ideal point resulting from areas of high $\dot{V}_A/\dot{Q}$, which are not included in the ideal A-aDO_2. However, these constructs share a high degree of commonality, and therefore, one would expect a strong relationship between the oxygen deficit and the ideal A-aDO_2. Prior studies (20) show this to be the case, with the r^2 of the correlation between A-aDO_2 and oxygen deficit in 23 patients being ~0.73.

In practice, the results from previous studies show that the oxygen deficit produces numbers that are physiologically reasonable. It is well established that in normal subjects without lung disease, the ideal A-aDO_2 is relatively small, and that this increases with healthy aging. When a cohort of normal subjects were tested, those categorized as "young" (19–31 yr) had a very low oxygen deficit (averaging 2.0 mmHg), whereas "older" (47–88 yr) subjects had an elevated value averaging 7.5 mmHg (19, 20). It is important to point out that these measurements were performed while the subjects were breathing a hypoxic gas mixture ($F_{I_{O_2}}$ 0.125) for at least 10 min to lower their otherwise normal fractional saturation values to a range where calculation of the arterial Pa_{O_2} from end-tidal measurements was practical. It is well known that for a given degree of $\dot{V}_A/\dot{Q}$ inequality in the lung, the A-aDO_2 will be lower at lower levels of inspired O_2 since the arterial point will be on a steeper part of the O_2-Hb dissociation curve than would be the case breathing a normoxic gas (15). Thus, the low values for the oxygen deficit in these two cohorts of normal subjects may result, at least in part, from the hypoxia imposed during measurement. Although this alters the absolute values, the effect is present in both the young and older cohorts, showing a clear effect of age on the oxygen deficit, as expected.

In contrast to the data from normal subjects, a cohort of patients with a range of pulmonary diseases breathing air ($F_{I_{O_2}}$ 0.21) show a much higher value for the oxygen deficit (averaging 41.9 mmHg) (20). All of these patients had fractional saturation values of 0.95 or less breathing air, and their calculated oxygen deficit was much higher than either normal cohort. In the patients studied, their underlying lung disease resulted in their oxygen saturation being ≤95% (they were selected based on this criterion), and so these measurements also occurred when they were operating on the steep potion of the O_2-Hb dissociation curve. Similarly, the patient cohort had (as expected) elevated A-aDO_2 values, and these are well correlated with the oxygen deficit values with an r^2 of ~0.73 (20).

Appropriateness of the Error Analysis

The Monte Carlo simulations we performed necessarily rest on the choices made in terms of the variability in the input parameters, end-tidal O_2, end-tidal CO_2, and fractional saturation. We based this on the observed variability in 37 subjects with ~16 measurements per subject spread across 4 values of $F_{I_{O_2}}$ (a total of 597 measurements). Thus, we have a high degree of confidence that the variability we used in the Monte Carlo simulations is representative of that seen in actual use. In the case of the end-tidal measurements, the observed variability in end-tidal O_2 is 3.3% (SD), which, assuming a respiratory exchange ratio of 0.8, would imply a variability in end-tidal CO_2 of 2.6%. The observed variability in end-tidal CO_2 was 2.7%, suggesting that it was appropriate to use the opposing direction variation in O_2 and CO_2 in our simulations. It should also be noted that the variability in oxygen deficit that results from variability in end-tidal O_2 would similarly affect direct measurements of the A-aDO_2 for which oxygen deficit is a surrogate.

The other input measurement is the fractional saturation. Pulse oximetry is subject to confounding issues that can serve to limit accuracy and reliability. We have no way to directly assess accuracy, and if there are influences that serve to make the measurement inaccurate [e.g., poor fingertip perfusion, the presence of Met-Hb, or manufacturing issues (8)], that will necessarily result in an error in oxygen deficit. Reliability, however, is addressed by the Monte Carlo simulations. A large meta-analysis study showed that most models of pulse oximeter were accurate within 2% (±1 SD) with fingertip probes (as used here) being superior to forehead probes (7). The observed variability in fractional saturation was 0.008 (SD), with slightly higher variability at lower values of fractional saturation. Based on that, we used an error in fractional saturation of 0.01 (SD) as an absolute value regardless of the underlying value of fractional saturation.

Fundamental Limitations

The calculation of the oxygen deficit has some limitations, and these should be considered when interpreting the results.

Validity of end-tidal gas a measure of alveolar concentration. It is assumed that the end-tidal gas concentrations measured in expired gas are reflective of the alveolar partial pressure of O_2 and CO_2. As expiration proceeds the expired value of O_2 falls, and the value of CO_2 rises resulting in the well-known sloping "alveolar plateau." The slope occurs for two reasons. First, continuing gas exchange means that as expiration proceeds, O_2 is removed from the alveoli, and CO_2 is added. The magnitude of this effect depends on metabolic rate and lung volume but has been shown to be responsible for only a small portion (~10%) of the alveolar plateau slope in single breath tests (4). Second, the greater contribution to the slope of the alveolar plateau results from asynchronous emptying of lung units with different $\dot{V}_A/\dot{Q}$ ratios (and thus with different values of O_2 and CO_2). This effect has been utilized to provide estimates of the degree of ventilation-perfusion inequality in the lung (17) and has been utilized in studies in situations where direct measurements of $\dot{V}_A/\dot{Q}$ inequality are not possible, such as diving (5) and spaceflight (10, 11). It has been shown to provide a good correlation with measured $\dot{V}_A/\dot{Q}$ inequality in animal studies (12). The implication of the majority of the observed alveolar plateau slope resulting from $\dot{V}_A/\dot{Q}$ inequality is that end-tidal gas values are affected by that inequality. However, since the value of O_2 continues to fall as expiration proceeds (and CO_2 continues to rise), this raises the question of the point in expiration that the continuously changing gas concentrations should be measured. Here, we use the end-tidal value, defined as the average of the gas concentration in the half-second preceding the onset of the following inspiration as the alveolar value. With the subject breathing quietly, expiration terminates at functional residual capacity, and this lung volume is highly reliable. We provide a trend plot (lower part of Fig. 1) as a visual indicator of the stability of end-tidal values of O_2 and CO_2 and average the last five values for use in calculating the oxygen deficit. Furthermore, by considering the variance of the end-tidal CO_2 values, we provide an indicator for the operator of whether the subject is in steady state. However, the instantaneous values of O_2 and CO_2 do not necessarily lie on the gas-R line (6) because of variations in expiratory flow sequencing, cardiogenic oscillations, and other factors. Such factors were not directly included in the Monte Carlo simulations, although the data on variability in end-tidal values likely include such effects. However, it remains possible that such deviations from the gas-R line have the potential to increase the variability in the measured oxygen deficit.

Error resulting from a nonzero base excess and temperature. Because the technique relies on noninvasive measurements, no correction for base excess (should any be present) is practical. A base excess of 10 mEq/L would result in an ~3 mmHg underestimation in P_{O_2}, raising the oxygen deficit by ~3 mmHg at a saturation of 90%. The effect is, however, asymmetric, and a base deficit of 10 mEq/L would lower oxygen deficit by ~8 mmHg.

Temperature also serves to alter the P50 of the O_2-Hb dissociation curve. A 2°C increase in body temperature would serve to lower the oxygen deficit by ~3.5 mmHg, all other factors being equal.

Both base excess and temperature are the two factors that have the potential to produce biases in oxygen deficit measurement. The effect of temperature could readily be accounted for, as the effect is essentially linear and independent of saturation. Accounting for base excess is more nuanced, although it might argued that subjects with a substantial alteration in their acid-base status would be more likely to have a significant gas exchange defect and thus have higher values of the oxygen deficit, making the effect of not accounting for base excess less of an issue.

Conclusion

A reliable and potentially valuable picture of the overall state of pulmonary gas exchange can be obtained from the combination of expired gas measurements and pulse oximetry. There are some limitations. The shape of the O_2-Hb dissociation curve, which is very flat at high values of P_{O_2}, means that the accuracy estimates of the oxygen deficit fall rapidly for values of fractional saturation of ~0.95 or above, and there is a negative bias in the calculated oxygen deficit resulting from a combination of underestimation in Pa_{O_2} from the Hill equation and an upper bound for the value of fractional saturation. Provided that the subject is in a steady state in terms of breathing pattern, then the measured end-tidal values for P_{O_2} and P_{CO_2} are adequate to account for the Bohr effect and to provide an end-tidal P_{O_2} that, when combined with the estimated arterial P_{O_2}, allows the oxygen deficit to be calculated. The errors that result if the base excess is not zero or body temperature is not 37°C are sufficiently small that useful results can still be obtained without measuring these. The result is that a valuable picture of pulmonary gas exchange can be obtained by having the patient breathe through a tube for a few minutes without the need for arterial blood gas sampling.

ACKNOWLEDGMENTS

We thank MediPines Corporation for the provision of prototype hardware used in the referenced studies. We thank Janelle Fine for work with the technical implementation of the early prototype devices and for assistance in data collection.

GRANTS

Financial support was provided by the University of California, San Diego.

DISCLOSURES

The University of California, San Diego has exclusively licensed technology to MediPines Corporation, Orange County, CA, to develop a device based on this work. J. B. West has a financial interest with MediPines Corporation.

AUTHOR CONTRIBUTIONS

G.K.P. and J.B.W. conceived and designed research; G.K.P. performed experiments; G.K.P. analyzed data; G.K.P. and J.B.W. interpreted results of experiments; G.K.P. prepared figures; G.K.P. drafted manuscript; G.K.P. and J.B.W. edited and revised manuscript; G.K.P. and J.B.W. approved final version of manuscript.

REFERENCES

1. **Anthonisen NR, Fleetham JA.** Ventilation: total, alveolar, and deadspace. In: *Handbook of Physiology. The Respiratory System. Gas Exchange*, edited by Farhi L, Tenney SM. Bethesda, MD: American Physiological Society, 1987, p. 113–129.
2. **Bates JH, Prisk GK, Tanner TE, McKinnon AE.** Correcting for the dynamic response of a respiratory mass spectrometer. *J Appl Physiol* 55: 1015–1022, 1983. doi:10.1152/jappl.1983.55.3.1015.
3. **Comroe JH Jr, Dripps RD Jr.** The oxygen tension of arterial blood and alveolar air in normal human subjects. *Am J Physiol* 142: 700–707, 1944. doi:10.1152/ajplegacy.1944.142.5.700.
4. **Cormier Y, Bélanger J.** Contribution of gas exchange to slope of phase III of the single-breath nitrogen test. *J Appl Physiol* 50: 1156–1160, 1981. doi:10.1152/jappl.1981.50.6.1156.
5. **Cotes JE, Davey IS, Reed JW, Rooks M.** Respiratory effects of a single saturation dive to 300 m. *Br J Ind Med* 44: 76–82, 1987. doi:10.1136/oem.44.2.76.
6. **DuBois AB, Britt AG, Fenn WO.** Alveolar CO2 during the respiratory cycle. *J Appl Physiol* 4: 535–548, 1952. doi:10.1152/jappl.1952.4.7.535.
7. **Jensen LA, Onyskiw JE, Prasad NG.** Meta-analysis of arterial oxygen saturation monitoring by pulse oximetry in adults. *Heart Lung* 27: 387–408, 1998. doi:10.1016/S0147-9563(98)90086-3.
8. **Milner QJ, Mathews GR.** An assessment of the accuracy of pulse oximeters. *Anaesthesia* 67: 396–401, 2012. doi:10.1111/j.1365-2044.2011.07021.x.
9. **Pickerodt PA, Kuebler WM.** Go West: translational physiology for noninvasive measurement of pulmonary gas exchange in patients with hypoxemic lung disease. *Am J Physiol Lung Cell Mol Physiol* 316: L701–L702, 2019. doi:10.1152/ajplung.00515.2018.
10. **Prisk GK, Elliott AR, Guy HJ, Kosonen JM, West JB.** Pulmonary gas exchange and its determinants during sustained microgravity on Spacelabs SLS-1 and SLS-2. *J Appl Physiol (1985)* 79: 1290–1298, 1995. doi:10.1152/jappl.1995.79.4.1290.
11. **Prisk GK, Fine JM, Cooper TK, West JB.** Vital capacity, respiratory muscle strength, and pulmonary gas exchange during long-duration exposure to microgravity. *J Appl Physiol (1985)* 101: 439–447, 2006. doi:10.1152/japplphysiol.01419.2005.
12. **Prisk GK, Guy HJ, West JB, Reed JW.** Validation of measurements of ventilation-to-perfusion ratio inequality in the lung from expired gas. *J Appl Physiol (1985)* 94: 1186–1192, 2003. doi:10.1152/japplphysiol.00662.2002.
13. **Riley RL, Cournand A.** "Ideal" alveolar air and the analysis of ventilation-perfusion relationships in the lung. *J Appl Physiol* 1: 825–847, 1949. doi:10.1152/jappl.1949.1.12.825.
14. **Severinghaus JW.** Blood gas calculator. *J Appl Physiol* 21: 1108–1116, 1966. doi:10.1152/jappl.1966.21.3.1108.
15. **West JB.** *Respiratory Physiology - The Essentials*. Baltimore: Lippincott Williams & Wilkins, 2012.
16. **West JB, Crouch DR, Fine JM, Makadia D, Wang DL, Prisk GK.** A new, noninvasive method of measuring impaired pulmonary gas exchange in lung disease: an outpatient study. *Chest* 154: 363–369, 2018. doi:10.1016/j.chest.2018.02.001.
17. **West JB, Fowler KT, Hugh-Jones P, O'Donnell TV.** Measurement of the ventilation-perfusion ratio inequality in the lung by the analysis of a single expirate. *Clin Sci* 16: 529–547, 1957.
18. **West JB, Wagner PD.** Pulmonary gas exchange. In: *Bioengineering Aspects of the Lung*. New York: Marcel Dekker, Inc, 1977, p. 361–457.
19. **West JB, Wang DL, Prisk GK.** Measurements of pulmonary gas exchange efficiency using expired gas and oximetry: results in normal subjects. *Am J Physiol Lung Cell Mol Physiol* 314: L686–L689, 2018. doi:10.1152/ajplung.00499.2017.
20. **West JB, Wang DL, Prisk GK, Fine JM, Bellinghausen A, Light M, Crouch DR.** Noninvasive measurement of pulmonary gas exchange: comparison with data from arterial blood gases. *Am J Physiol Lung Cell Mol Physiol* 316: L114–L118, 2019. doi:10.1152/ajplung.00371.2018.